

Enforcing KL Regularization in General Tsallis Entropy Reinforcement Learning via Advantage Learning

Lingwei Zhu¹

Zheng Chen²

Eiji Uchibe³

Takamitsu Matsubara¹

¹Nara Institute of Science and Technology, Japan

²Osaka University, Japan

³Advanced Telecommunication Research, Japan

Abstract

Maximum Tsallis entropy (MTE) framework in reinforcement learning has gained popularity recently by virtue of its flexible modeling choices including the widely used Shannon entropy and sparse entropy. However, non-Shannon entropies suffer from approximation error and subsequent underperformance either due to its sensitivity or the lack of closed-form policy expression. To improve the tradeoff between flexibility and empirical performance, we propose to strengthen their error-robustness by enforcing implicit Kullback-Leibler (KL) regularization in MTE motivated by Munchausen DQN (MDQN). We do so by drawing connection between MDQN and advantage learning, by which MDQN is shown to fail on generalizing to the MTE framework. The proposed method Tsallis Advantage Learning (TAL) is verified on extensive experiments to not only significantly improve upon Tsallis-DQN for various non-closed-form Tsallis entropies, but also exhibits comparable performance to state-of-the-art maximum Shannon entropy algorithms.

1 INTRODUCTION

The successes of modern reinforcement learning (RL) rely crucially on implementing value-based methods with powerful function approximators [Mnih et al., 2015, Andrychowicz et al., 2020]. However, the susceptibility of value-based methods is also magnified: various sources of error can perturb action value estimates such that the non-optimal actions have temporally higher values than the optimal ones, putting unit probability mass on such deceptive actions can greatly slow down learning [Fujimoto et al., 2018, Fu et al., 2019] or even cause divergence [Bertsekas and Tsitsiklis, 1996, Wagner, 2011, Bellemare et al., 2016].

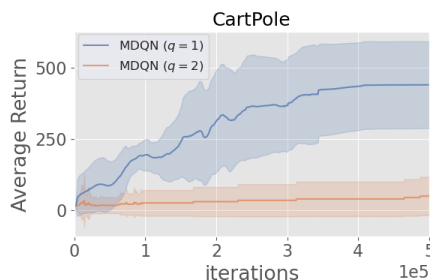


Figure 1: Munchausen DQN (MDQN) with entropic indices $q = 1, 2$ (defined in Section 3). For $q \neq 1$ MDQN failed to learn anything on the simple environment `CartPole-v1`.

Recently there has seen promising progress towards alleviating this problem by leveraging *entropy-regularized* algorithms [Haarnoja et al., 2018, Ahmed et al., 2019]: by introducing entropy the policy becomes stochastic, hence optimal actions with temporarily low values can still be selected and subsequently help correct the value estimate. Besides the well-known Shannon entropy giving rise to Boltzmann softmax policy, the maximum Tsallis entropy (MTE) framework has gained recent popularity in that it offers more flexible modeling choices: by varying its entropic index q , Shannon entropy ($q = 1$) and Tsallis sparse entropy ($q = 2$) [Martins and Astudillo, 2016, Lee et al., 2018] can be recovered [Lee et al., 2020]. Other values between $1 < q < 2$ and $q > 2$ can also serve as an interesting substitute to Shannon or sparse entropy for more compact/diverse policies. However, a common problem of those entropies is the lack of robustness against errors: they do not enjoy closed-form policy expression when $q \neq 1, 2$, hence empirical underperformance is often incurred by significant greedy step error. The sensitivity to errors holds true even for the closed-form sparsemax policy ($q = 2$): due to its compactness, by contrast it is inherently less robust than the softmax [Chen et al., 2018, Lee et al., 2020].

Implicit Kullback-Leibler (KL) regularization might come to rescue for improving the error-robustness of non-Shannon

entropies. Currently one of the state-of-the-art methods Munchausen Deep Q-Network (MDQN) [Vieillard et al., 2020b] has demonstrated that significant performance boost can be attained by adding logarithm of the stochastic policy $\ln \pi$ as a bootstrapping term to any temporal difference learning algorithms for facilitating learning. The general claim and success of MDQN motivates us to investigate its Munchausen Tsallis DQN counterpart. However, as shown in Figure 1, MDQN typically fails to learn anything even for simple tasks with Tsallis entropy when $q \neq 1$, which suggests that directly resorting to MDQN for Tsallis entropy is infeasible.

In this paper, we connect three relevant ideas: MDQN, KL regularization and advantage learning. We show the implicit KL regularization of MDQN happens as a result of advantage learning which is due to the equivalence between log-policy and advantage function, which only holds for Shannon entropy $q = 1$. Therefore, the failure of MDQN in MTE is expected since for $q \neq 1$ the equivalence is lost. Motivated by this observation, we propose to enforce implicit KL regularization by explicitly enlarging the action gap in the MTE framework. By extensive experiments we demonstrate that TAL achieves significant improvement over the state-of-the-art value-based MTE method Tsallis-DQN, even for those entropic indices that do not have closed-form policy expression. We also show its performance is competitive with state-of-the-art advantage learning algorithms (including original MDQN), which brings a competitive substitute for the conventional Shannon entropy in relevant domains [Lee et al., 2020].

The rest of the paper is organized as follows: in Section 2 we briefly survey related work. In Section 3 we review the background for the proposed method in Section 4. The proposed framework is comprehensively evaluated in Section 5. We conclude the paper in Section 6.

2 RELATED WORK

The very recent success of MDQN shows significantly improved performance can be attained by simply augmenting reward function with logarithm of the policy. While the authors of [Vieillard et al., 2020b] claimed such log-policy augmentation is generally applicable for any stochastic policy and demonstrated the effectiveness for soft Q-learning, we found that in practice MDQN worked poorly with the more general Tsallis entropy that is more suited to risk-sensitive applications [Lee et al., 2018, 2020], which begs the question of why MDQN achieved superior performance only with Shannon entropy. The connection with action gap maximization was mentioned in [Vieillard et al., 2020b], though the authors attributed the superior performance of MDQN to implicit KL regularization.

The concept of advantage learning due to [Baird and Moore,

1999] lies in increasing the action gap and hence increasingly distinguishing the optimal action from suboptimal ones. Besides rendering the algorithm empirically more robust, increased action gap comes with various benefits. For example, Farahmand [2011] showed that if the action gap regularity assumption holds, convergence rate of suboptimality gap towards zero can be much faster. Bellemare et al. [2016] studied the non-stationary policy problem of Bellman optimality operator and proposed a solution by modifying based on the advantage learning scheme. Recently, advantage learning was extended by [Lu et al., 2019] to the setting of random action gap coefficients and by [Ferret et al., 2021] to self-imitation learning.

The connection between advantage learning and entropy-regularized RL was first alluded to by [Azar et al., 2012] when studying KL-regularized policy iteration. This approach was followed by [Kozuno et al., 2019] to incorporate Shannon entropy. By defining a preference function, Kozuno et al. [2019] found that KL regularization is possible by iterating upon an advantage learning scheme. In [Vieillard et al., 2020b], the authors showed how to derive CVI starting from MDQN. In this paper, we derive MDQN from CVI from an advantage learning perspective. By connecting those ideas we justify the use of advantage learning for implicitly enforcing KL regularization in the MTE framework.

3 BACKGROUND

3.1 RL BASICS

Reinforcement learning problems are typically formulated by Markov decision processes (MDPs) which are expressed by the quintuple $(\mathcal{S}, \mathcal{A}, P, r, \gamma)$, where \mathcal{S} and \mathcal{A} denote state space and action space, respectively. $|\mathcal{S}|$ defines the cardinality of state space and likewise for the action space. P denotes the transition probability kernel such that $P(\cdot|s, a)$ indicates the probability of transitioning to next state conditional upon taking action a in state s . Let $r(s, a)$ denote the reward associated with that transition. When the time dependence t should be made explicit, we write $r_t := r(s_t, a_t)$. The discount factor $\gamma \in (0, 1)$ trades off the importance between current and future rewards. A policy π maps a state to a distribution over actions. We define the state-action value function $Q_\pi \in \mathbb{R}^{|\mathcal{S}| \times |\mathcal{A}|}$ as:

$$Q_\pi(s, a) = \mathbb{E} \left[\sum_{t=0}^{\infty} \gamma^t r_t | s_0 = s, a_0 = a \right], \quad (1)$$

where the expectation is with respect to the trajectory induced by policy π and transition probability P .

Value-based methods typically iterate on an initial Q as: $T_\pi Q := r + \gamma P_\pi Q$, where T_π denotes the Bellman operator and $\gamma P_\pi Q := \gamma \mathbb{E}_{s' \sim P(\cdot|s, a), a' \sim \pi(\cdot|s')} [Q(s', a')]$, with the definition being component-wise. Repeating the above it-

eration guarantees convergence to its unique fixed point Q_π . Our goal is to find an optimal policy π^* such that $T_*Q = \max_\pi T_\pi Q$. The optimal policy can be extracted with the greedy operator $\pi(a|s) = \mathcal{G}(Q_\pi) := \arg \max_\pi Q_\pi$. For convenience, for any two functions $F_1, F_2 \in \mathbb{R}^{|S| \times |A|}$ we define their inner product as $\langle F_1, F_2 \rangle \in \mathbb{R}^{|S|}$. We also define $\mathbf{1}$ as an all-one vector whose dimension should be clear from the context.

To render the policy robust against suboptimal actions that have temporally deceptively high values, advantage learning scheme augments the standard Bellman operator $T_\pi Q$ with an additional action gap or advantage function: $A_\pi \in \mathbb{R}^{|S| \times |A|} = Q_\pi - V_\pi$, where $V_\pi = \langle \pi, Q_\pi \rangle$ is the average of action values. The agent is prompted to select actions that have values higher than the average to increasingly distinguish optimal actions from bad ones.

3.2 MAXIMUM ENTROPY RL

In the recently popular maximum entropy RL literature, the reward is augmented by the Shannon entropy $\tau \mathcal{H}(\pi) := \tau \langle -\pi, \ln \pi \rangle$, where τ is the augmentation coefficient. By the Fenchel conjugacy [Geist et al., 2019], the Shannon entropy induced optimal policy is a Boltzmann distribution:

$$\mathcal{G}^\tau(Q) = \frac{\exp(\tau^{-1}Q)}{\langle \mathbf{1}, \exp(\tau^{-1}Q) \rangle} = \exp(\tau^{-1}(Q - V)), \quad (2)$$

$V := \tau \ln \langle \mathbf{1}, \exp(\tau^{-1}Q) \rangle$ is the soft value function. Its regularized Bellman operators are defined as $T_\pi^\tau Q = r + \gamma P \langle \pi, Q - \tau \ln \pi \rangle$.

It turns out that the Shannon entropy is a special case of the well-known Tsallis entropy [Tsallis, 1988] parametrized by entropic index q :

$$\alpha H_q(\pi) := \alpha \frac{k}{q-1} (1 - \langle \mathbf{1}, \pi^q \rangle), \quad (3)$$

where α is its regularization coefficient. The Shannon entropy is recovered by letting $k = \frac{1}{2}$ and $q \rightarrow 1$. When $q \rightarrow \infty$, the regularization effect vanishes. In this paper, we fix $k = \frac{1}{2}$ and consider various cases of q . The corresponding regularized Bellman operator is hence given by $T_\pi^\alpha Q = r + \gamma P \langle \pi, Q + \frac{\alpha}{2(q-1)} (1 - \pi^{q-1}) \rangle$. Tsallis entropy induces the stochastic optimal policy as:

$$\mathcal{G}^\alpha(Q)(a|s) = \frac{\sqrt[q-1]{\left[\frac{Q(s,a)}{\alpha} - \psi \left(\frac{Q(s,\cdot)}{\alpha} \right) \right]_+}}{\sum_{a \in S(s)} \frac{\sqrt[q-1]{\left[\frac{Q(s,a)}{\alpha} - \psi \left(\frac{Q(s,\cdot)}{\alpha} \right) \right]_+}}}{q}, \quad (4)$$

where the operation $[\cdot]_+$ converts negative components to 0. ψ is the normalization term to ensure the policy sums to one. When $q = 2$, we recover the sparsemax policy [Lee et al., 2018, Chow et al., 2018] whose normalization is:

$$\psi \left(\frac{Q(s,\cdot)}{\alpha} \right) = \frac{\sum_{a \in S(s)} \frac{Q(s,a)}{\alpha} - 1}{K(s)}, \quad (5)$$

where $S(s)$ is the set of actions satisfying $1 + i \frac{Q(s,a(i))}{\alpha} > \sum_{j=1}^i \frac{Q(s,a(j))}{\alpha}$, $a(j)$ indicates the action with j th largest action value, $K(s)$ denotes the cardinality of $S(s)$. The value function is

$$V = \frac{1}{2} \sum_{j=1}^{K(s)} \left(\left(\frac{Q(s,a(j))}{\alpha} \right)^2 - \psi \left(\frac{Q(s,\cdot)}{\alpha} \right)^2 \right) + \frac{1}{2}. \quad (6)$$

The sparsemax policy has been recently demonstrated as a suitable candidate for safety-sensitive tasks such as robotics [Lee et al., 2018, 2020]. However, the performance of its value-based methods typically cannot match Shannon entropy since it often results in insufficient exploration.

When $q \neq 1, 2, \infty$, the normalization term and hence optimal policy might not have closed-form expression. But we can approximate the optimal policy by leveraging first order expansion following [Chen et al., 2018]¹:

$$\tilde{\mathcal{G}}^\alpha(Q)(a|s) \approx \sqrt[q-1]{\left[\frac{Q(s,a)}{\alpha} - \tilde{\psi} \left(\frac{Q(s,\cdot)}{\alpha} \right) \right]_+}, \quad (7)$$

where $\tilde{\psi} \left(\frac{Q(s,\cdot)}{\alpha} \right) \approx \frac{\sum_{a \in S(s)} \frac{Q(s,a)}{\alpha} - \frac{1}{2}q}{K(s)} + \left(\frac{q}{2} - \frac{q}{q-2} \right)$ is the approximate normalization. The set $S(s)$ then allows actions satisfying $\frac{1}{2}q + i \frac{Q(s,a)}{\alpha} > \sum_{j=1}^i \frac{Q(s,a(j))}{\alpha} + j \left(\frac{q}{2} - \frac{q}{q-2} \right)$. We denote its associated Bellman operator as \tilde{T}_π^α . Detailed derivation of approximate Tsallis policy is left to Appendix A.

4 APPROACH

4.1 MUNCHAUSEN RL

MDQN [Vieillard et al., 2020b] proposes *optimizing for the immediate reward augmented by the scaled log-policy of the agent when using any TD scheme*. Specifically, MDQN was implemented based on soft Q-learning as follows:

$$\begin{cases} \pi_{k+1} = \arg \max_\pi \langle \pi, Q_k \rangle + \tau \mathcal{H}(\pi) \\ Q_{k+1} = r + \beta \tau \ln \pi_{k+1} + \gamma P \langle \pi_{k+1}, Q_k - \tau \ln \pi_{k+1} \rangle \end{cases}, \quad (8)$$

where the red term is the *Munchausen term*, the blue term comes from soft Q-learning. For simplicity let $\beta = 1$, MDQN has the following equivalence:

$$\begin{aligned} Q_{k+1} - \tau \ln \pi_{k+1} &= \\ r + \gamma P (\langle \pi_{k+1}, Q_k - \tau \ln \pi_k \rangle - \tau D_{KL}(\pi_{k+1} || \pi_k)) & \\ \Leftrightarrow Q'_{k+1} = r + \gamma P (\langle \pi_{k+1}, Q'_k \rangle - \tau D_{KL}(\pi_{k+1} || \pi_k)), & \end{aligned} \quad (9)$$

¹Chen et al. [2018] considered the case of $k = 1$, while we consider $k = \frac{1}{2}$ in this paper.

where $Q'_k := Q_k - \tau \ln \pi_k$ is the newly defined action value function. Hence MDQN performs KL regularization by adding the Munchausen term $\ln \pi_{k+1}$ to soft Q-learning. One of the crucial properties of KL regularization is its optimal policy averages over past action values: $\pi_{k+1} \propto \exp\left(\tau^{-1} \sum_{j=1}^k Q_j\right)$ [Vieillard et al., 2020a], which effectively cancels out errors under mild assumptions.

In the following section, we show the implicit KL regularization is performed when the Munchausen term $\ln \pi$ is equivalent to performing advantage learning under certain conditions, motivating our later proposal.

4.2 AN ADVANTAGE LEARNING PERSPECTIVE FOR MUNCHAUSEN RL

It is worth noting that in the lieu of Shannon entropy augmentation, from Eq. (2) one has $\ln \pi = \tau^{-1}(Q - V)$, hence adding the Munchausen term coincides with advantage learning. In the recent literature, conservative value iteration (CVI) [Kozuno et al., 2019] comprehensively analyzes the relationship between advantage learning and KL regularization: CVI states the conditions under which advantage learning could implicitly perform KL regularization.

The connection between MDQN, KL regularization and advantage learning motivates us to investigate the possibility of enforcing implicit KL regularization for the MTE framework via advantage learning. To do so, we need to verify that the superior performance of MDQN is due to advantage learning. We re-derive MDQN by manipulating the CVI update rule since CVI generalizes advantage learning. We provide full derivation in Appendix A.2 and succinctly summarize the key steps here.

It turns out the CVI update rule can be written as the following, with Ψ, W being the CVI action and state value function, respectively:

$$\Psi_{k+1} = r + \gamma P \langle \pi_{k+1}, \Psi_k \rangle + \beta (\Psi_k - W_k), \quad (10)$$

where $\beta \in [0, 1]$ is a function of the Shannon entropy and KL divergence coefficients.

It is worth noting that Eq. (10) is itself a new value iteration scheme **regardless of the definition** of Ψ and π since we can arbitrarily initialize Ψ_0, π_0 . CVI states that, if the policy π_{k+1} in Eq. (10) meets the Boltzmann assumption $\pi_{k+1} \propto \exp(\tau^{-1} \Psi_k)$ (CVI itself uses Boltzmann policy but analyzes general advantage learning), then iterating upon Eq. (10) along results in KL regularization.

The simplest method to ensure π_{k+1} is Boltzmann is perhaps to perform soft Q-learning. By rewriting Eq. (10) as a soft Q-learning scheme and replacing Ψ, W with Q, V we have:

$$Q_{k+1} = r + \beta(Q_k - V_k) + \gamma P \langle \pi_{k+1}, Q_k - \tau \ln \pi_{k+1} \rangle,$$

Algorithm 1: TAL-DQN

Input: total steps T , update period I , interaction period C , epsilon-greedy threshold ϵ
Initialize: Network weights $\theta = \theta$,
 Replay buffer $B = \{\}$
 1 **for** $t = 1, 2, \dots, T$ **do**
 2 Collect tuple (s_t, a_t, r_t, s_{t+1}) in B with $\pi_{q, \epsilon}$
 3 **if** $\text{mod}(t, C) = 0$ **then**
 4 | update θ with minibatch $B_t \subset B$ on \mathcal{L}_{TAL}
 5 **end**
 6 **if** $\text{mod}(t, I) = 0$ **then**
 7 | update target network $\bar{\theta} \leftarrow \theta$
 8 **end**
 9 **end**

where the blue part comes from soft Q-learning and the we recognize the red part is $\beta(Q_k - V_k) = \beta\tau \ln \pi_k$. We hence see this scheme is same with the MDQN update rule Eq. (8).

This above analysis implies that MDQN achieves implicit KL regularization and superior performance thanks to the equivalence between the Munchausen term and the action gap. This intuition is confirmed by that in practice, MDQN actually computes the $\ln \pi$ term by $Q - V$ [Vieillard et al., 2020b, Appendix B.1]. Hence as learning proceeds, the probabilities of optimal actions increase and so do $\ln \pi$, which implies the action gap is also increased as is shown in Figure 5.

The key for deriving the relationship between CVI and MDQN is the equivalence $\tau \ln \pi_{k+1} = Q_k - V_k$. It is hence natural to conjecture that, if the equivalence does not hold as when $q \neq 1$ in the general Tsallis entropy, MDQN can no longer perform implicit KL regularization, and learning performance might be significantly degraded. As an example, consider Eq. (4) which is $q=2$. The Munchausen term $\ln \pi = \ln \left[\frac{Q(s,a)}{\alpha} - \psi \left(\frac{Q(s,\cdot)}{\alpha} \right) \right]_+$ may be undefined since the policy assigns zero probabilities to some of the actions. Even if we add some small value Δ in practice to prevent ill-defined $\ln \pi$, it does not encode action gap information since $\alpha \ln \pi = \alpha \ln \left[\frac{Q(s,a)}{\alpha} - \psi \left(\frac{Q(s,\cdot)}{\alpha} \right) + \Delta \right]_+ \neq Q - V + \Delta$, where V was defined in Eq. (6). This conclusion holds for other q as well. Hence it is confirmed that resorting to MDQN does not bring KL regularization for the MTE framework.

4.3 ADVANTAGE LEARNING FOR GENERAL TSALLIS ENTROPY RL

Motivated by the observation in the prior section, instead of relying on $\ln \pi$, we propose to explicitly perform advantage learning by increasing the action gap $Q - \langle \pi, Q \rangle$ to conform to the advantage learning scheme of [Azar et al.,

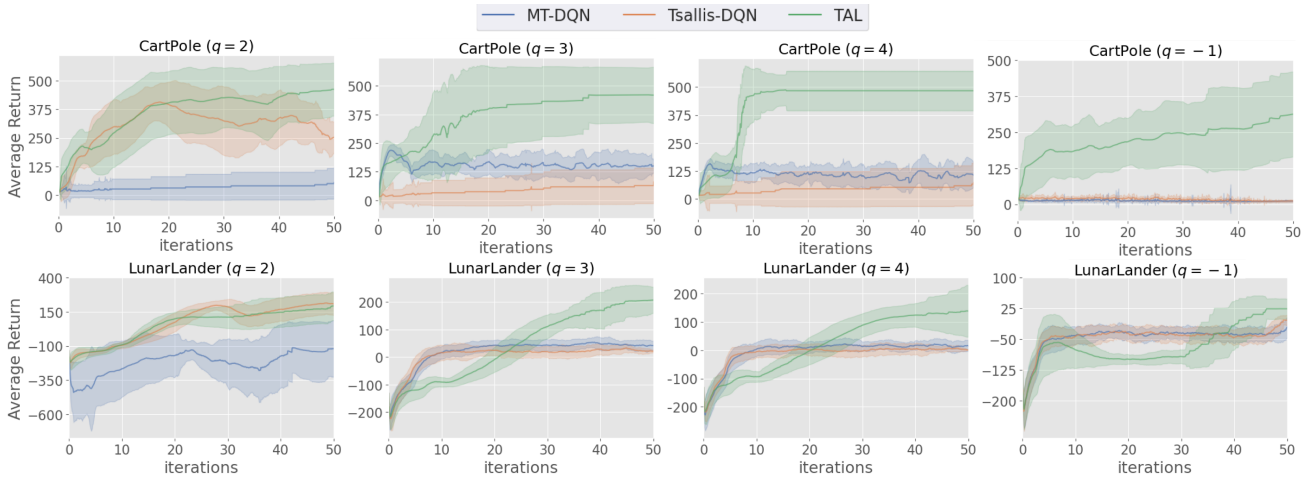


Figure 2: Comparison on `CartPole-v1` and `LunarLander-v2` between Tsallis Advantage Learning (TAL), Munchausen Tsallis DQN (MT-DQN) and Tsallis DQN with different entropic indices. All algorithms are averaged over 30 seeds to plot mean and ± 1 standard deviation. For $q = -1, 3, 4$, approximate policy in Eq. (7) is employed. When $q \leq 0$ Tsallis entropy becomes convex, hence the regularization properties fail to hold. We show $q = -1$ for completeness.

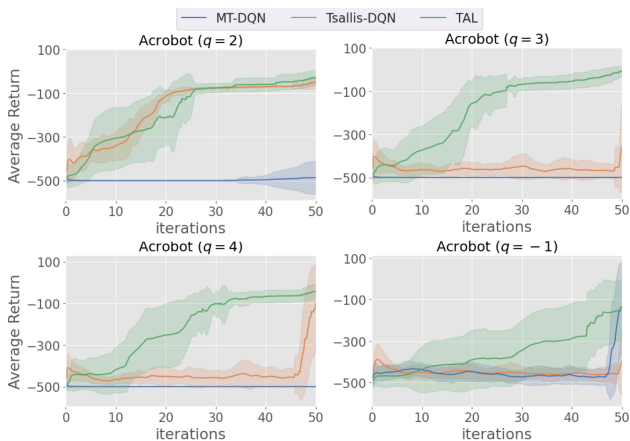


Figure 3: Comparison between Tsallis-DQN (orange), MT-DQN (blue) and TAL (green) with entropic indices $q = -1, 2, 3, 4$ on `Acrobot-v1`.

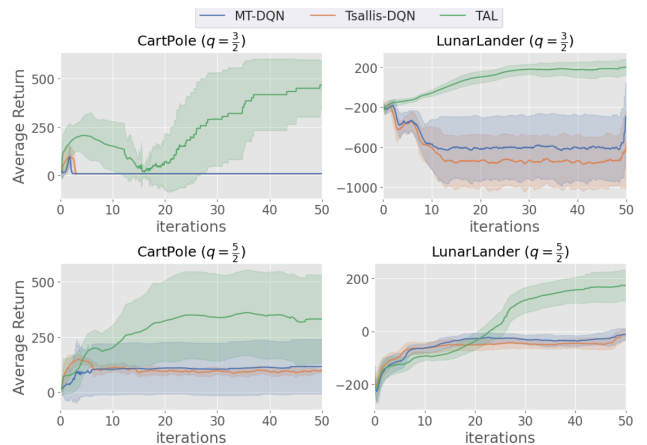


Figure 4: Comparison between Tsallis-DQN (orange), MT-DQN (blue) and TAL (green) with entropic indices $q = \frac{3}{2}, \frac{5}{2}$ on `CartPole-v1` and `LunarLander-v2`.

2012, Kozuno et al., 2019]. Though the policy with $q \neq 1$ is no longer Boltzmann, by [Kozuno et al., 2019, Eq. (12)] the Tsallis policy can still be used. For justification the reader is referred to Appendix A.3.

We can succinctly summarize the proposed method: Tsallis advantage learning (TAL) as the following:

$$\begin{cases} \pi_{k+1} = \tilde{\mathcal{G}}^\alpha(Q_k), \\ Q_{k+1} = (\tilde{T}_{\pi_{k+1}}^\alpha)^m Q_k + \beta(Q_k - \langle \pi_{k+1}, Q_k \rangle), \end{cases} \quad (11)$$

where $\tilde{\mathcal{G}}^\alpha$ is the approximate Tsallis policy defined in Eq. (7). We can also change the policy/Bellman operator pair $(\tilde{\mathcal{G}}^\alpha, T_\pi^\alpha)$ to $(\mathcal{G}^\tau, T_\pi^\tau), (\mathcal{G}^\alpha, T_\pi^\alpha), (\mathcal{G}, T_\pi)$ which correspond to setting $q = 1, 2, \infty$, respectively. When $q = 1$, this scheme coincides with Munchausen RL. When $q = \infty$, there

is no regularization hence the scheme degenerates to advantage learning [Baird and Moore, 1999]. The superscript m indicates m times application of the Bellman operator. Typically $m = 1, \infty$ which correspond to value iteration and policy iteration schemes. β is the advantage coefficient and typically is between $[0, 1]$. $\langle \pi_{k+1}, Q_k \rangle$ is used to approximate the regularized value function V . We found that this approximation led to significantly better performance.

In this paper we are interested in verifying effectiveness of the proposed method as a value iteration algorithm, i.e. $m = 1$. Specifically, we follow [Vieillard et al., 2020b] to implement our algorithm based on the DQN architecture. We maintain two networks with parameters $\theta, \hat{\theta}$, with the latter being target network updated after a fixed number of

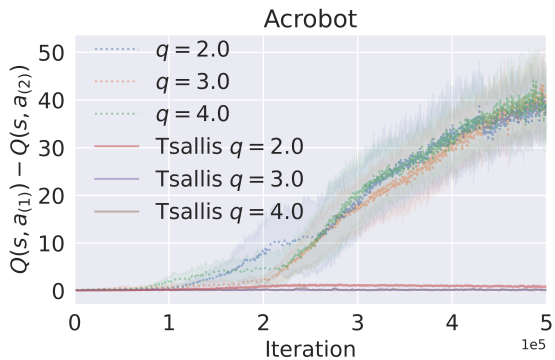


Figure 5: Action gap between the actions having the largest and second largest values $Q(s, a_{(1)}) - Q(s, a_{(2)})$ of TAL and Tsallis-DQN with different entropic indices.

timesteps. The loss function is defined by:

$$\mathcal{L}_{\text{TAL}}(\theta) := \hat{\mathbb{E}}_B \left[(r + \gamma \langle \pi_{\bar{\theta}}, Q_{\bar{\theta}} \rangle + \beta (Q_{\bar{\theta}} - \langle \pi_{\bar{\theta}}, Q_{\bar{\theta}} \rangle) - Q_{\theta})^2 \right],$$

where the policy $\pi_{\bar{\theta}}$ is computed following Eq. (11). The algorithm Tsallis Advantage Learning - DQN (TAL-DQN) is listed in Alg. 1. We provide implementation details in Appendix B.

5 EXPERIMENTS

We aim to demonstrate that the proposed algorithm TAL is an effective generalization of Munchausen RL, in that when entropic index $q = 1$ they coincide, but for other q the Munchausen bootstrapping term $\ln \pi$ can significantly deteriorate learning, while TAL can effectively boost the performance even for those q that entail approximation.

For comprehensive evaluation, we select three different domains: simple Gym classic control [Brockman et al., 2016], lightweight Atari games [Young and Tian, 2019] and challenging full-fledged Atari games [Bellemare et al., 2013]. We aim to show TAL improves upon the SOTA value-based Tsallis entropy method Tsallis-DQN and achieves comparable performance with SOTA advantage learning methods.

5.1 GYM CLASSIC CONTROL

We first examine the simple Gym classic control problems `CartPole-v1`, `LunarLander-v2` and `Acrobot-v1`. Their simplicity allows for evaluation with large number of seeds to verify our analysis. We name the algorithm Tsallis-DQN that sets $\beta = 0$ in Eq. (11) and compare Tsallis-DQN with TAL and Munchausen-Tsallis-DQN (MT-DQN) for entropic indices $q = -1, 2, 3, 4$. When $q = 2$ the policy has closed-form solution, for other indices the approximation introduced in Eq. (7) is employed. All algorithms are evaluated for 5×10^5 steps with 30 seeds. We decompose the

5×10^5 steps into 50 iterations. Implementation details such as network architecture and hyperparameters are provided in Appendix B.1. The results are shown in Figure 2.

Consistent with our analysis, Munchausen RL did not improve the performance for all entropic indices. For $q = 2$, MT-DQN failed to learn any meaningful behavior even with analytic policy expression, while Tsallis-DQN performed relatively well. For $q = 3, 4$, both MT-DQN and Tsallis-DQN failed to solve the `CartPole` environment. It is also interesting to inspect the case of $q = -1$, in which the Tsallis entropy becomes convex and hence the existing regularization results [Geist et al., 2019, Li et al., 2019] fail to hold. We show such result only for completeness, and one can expect the poor performance of all entropy-regularized algorithms. One can see the same trend holds true for `LunarLander-v2` and `Acrobot-v1` as well in Figure 3. We quantitatively evaluate the action gap between the actions with the largest and second largest values, i.e. $Q(s, a_{(1)}) - Q(s, a_{(2)})$ and show the averaged results in Figure 5, which proves that the action gap is indeed enlarged.

One might also be interested in non-integer value of q , since we might benefit from the intermediate values from the two analytic choices $q = 1, 2$. We therefore include the experiments with $q = \frac{3}{2}, \frac{5}{2}$ and show them in Figure 4. It is apparent that that the trend still holds valid for non-integer values of q . For $q = \frac{3}{2} \in [1, 2]$, we can expect this choice induces policy that stands between the softmax ($q = 1$) and the Sparsemax ($q = 2$), in that it is neither sparse nor assigns probability to all actions. However, with this choice, on both environments Tsallis-DQN and MT-DQN performed extremely poor, leading to the lowest scores possible. On the other hand, TAL managed to robustly converge to the optimal policy.

For $q = \frac{5}{2}$ the situation is similar, with small improvement of Tsallis-DQN and MT-DQN. But we can see TAL did not converge to the optimal solution on `CartPole-v1`, this might be due to the hyperparameters in Table 1 requires further fine-tuning for such specific choice.

5.2 MINATAR GAMES

We inspect whether TAL can still boost the performance of Tsallis-DQN and work well on relatively complicated problems with high dimensional image as the state space. MinAtar provides 5 lightweight Atari games with optimization on multiple aspects including sticky actions, training frequency and reward normalization, etc. We compare TAL with Tsallis-DQN, MT-DQN with entropic index $q = 2$ since it enjoys closed-form policy expression. We also compare with persistent AL (PAL) [Bellemare et al., 2016] that corrects the bias of the Bellman optimality operator; stochastic AL (SAL) that generalizes β to random variables drawn from various distributions [Lu et al., 2019]. Every run con-

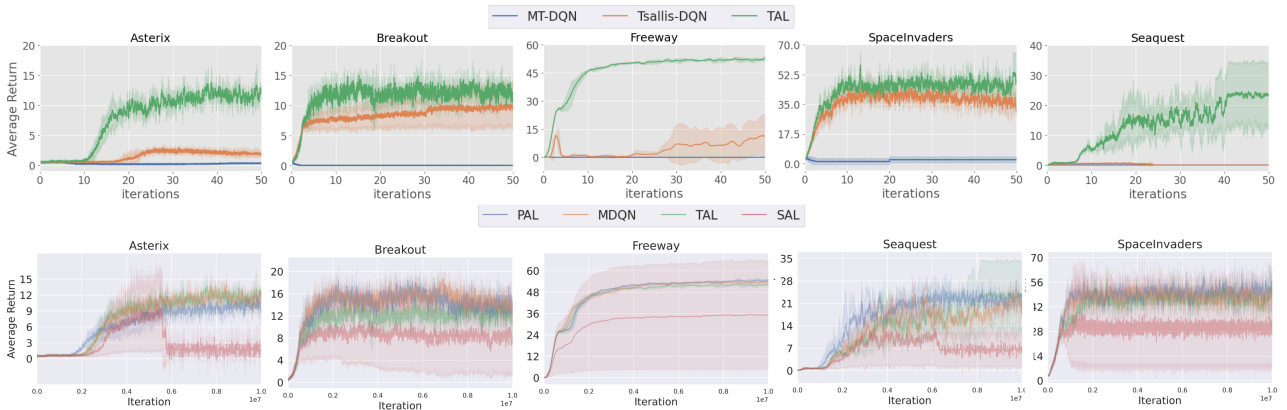


Figure 6: (Upper) Comparison between TAL, Tsallis-DQN and MT-DQN for $q=2$ on all MinAtar games. (Lower) Comparison between TAL, Munchausen-DQN (MDQN), Persistent AL (PAL) and Stochastic AL (SAL) on all MinAtar games. All algorithms are averaged over 3 seeds to plot mean and ± 1 standard deviation.

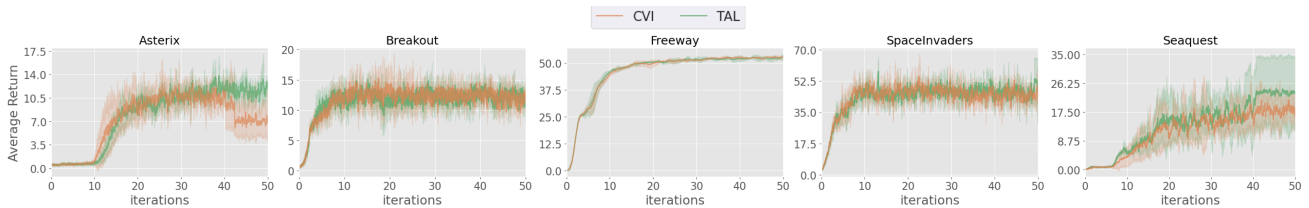


Figure 7: Comparison between conservative value iteration (CVI) and TAL ($q=2$) on all MinAtar games. The similar learning curves indicate TAL can achieve performance comparable to SOTA algorithms but with more desirable properties such as sparsity or parsimonious description of actions.

sists of 10^7 frames without frame skipping. We define every 200,000 frames as one iteration so totally 50 iterations. All algorithms are averaged over 3 seeds. Since we use image as input, convolutional network is necessary. We detail the network architecture and hyperparameters used for all algorithms in Appendix B.2.

We first examine whether TAL boosts the performance of Tsallis-DQN. From the upper row of Figure 6 it is clear that for relatively simple environments like Breakout and SpaceInvaders, TAL improved upon Tsallis-DQN slightly. However for challenging tasks like Seaquest, Asterix, Freeway, Tsallis-DQN failed to learn meaningful behavior while TAL successfully converged. By contrast, MT-DQN showed flat learning curves for all environments, validating our analysis that $\ln \pi$ does not encode action gap information and hence can deteriorate learning.

We also ask whether TAL can compete with state-of-the-art advantage learning algorithms. It is known that the hard max policy induced by Tsallis sparse entropy might cause brittle value function during learning, typically the performance of Tsallis entropy regularized algorithms cannot match SOTA algorithms such as PAL. From the lower row of Figure 6 we can see that PAL and MDQN performed the best, but TAL had similar performance throughout.

On the other hand, SAL with the empirically performant choice of β failed to keep up with other three algorithms due to the strong stochasticity in the advantage coefficient. This section confirms that Tsallis entropy regularized algorithms can perform competitively with SOTA advantage learning algorithms while enjoying strong theoretical properties for policies, whose good performance was due to the advantage learning and subsequent implicit KL regularization.

5.3 DISTRIBUTIONAL TAL ON ATARI GAMES

Similar to Munchausen RL that can be combined with distributional RL methods. We demonstrate that TAL can also be leveraged in the context of distributional RL. Specifically, we implement TAL on top of the *quantile regression DQN* (QR-DQN) [Dabney et al., 2018].

We compare TAL with MT-DQN with entropic index $q=2$, since $q=1$ coincides with MDQN. We choose a subset of 15 games from the full-fledged Atari games [Bellemare et al., 2013] for showing TAL remains effective for challenging problems. Implementation details are provided in Appendix B.3. Every single run consists of 3×10^7 steps. We define every 10^5 steps as one iteration so totally 300 iterations. All algorithms are averaged over 3 seeds.

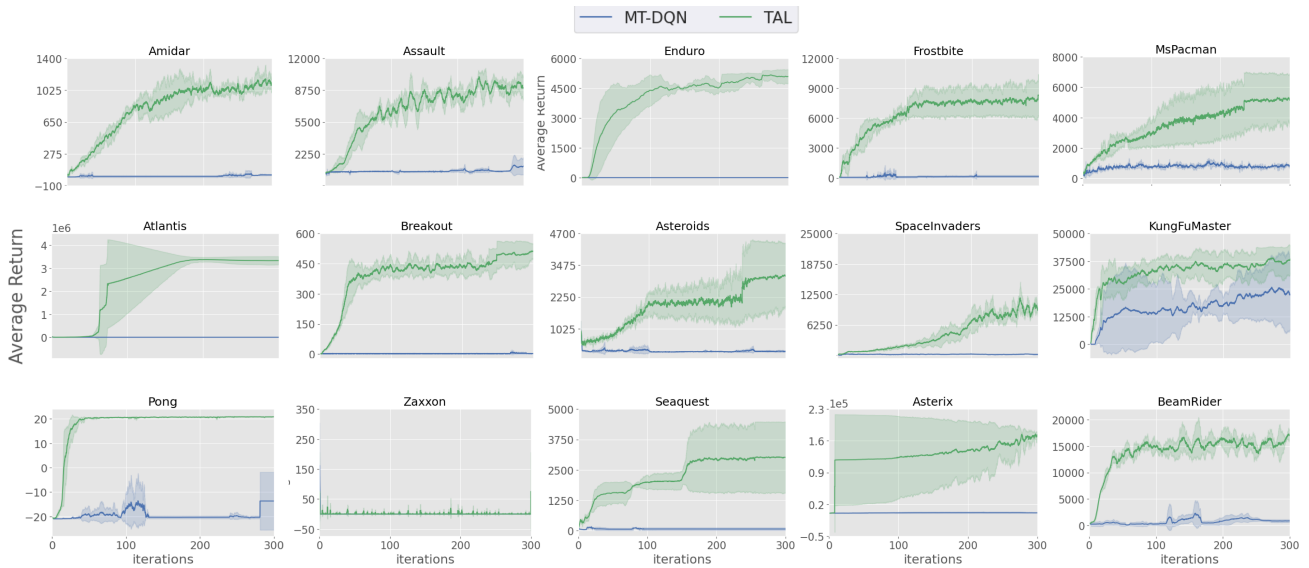


Figure 8: Comparison on full-fledged Atari games between TAL and MT-DQN implemented based on QR-DQN for $q = 2$.

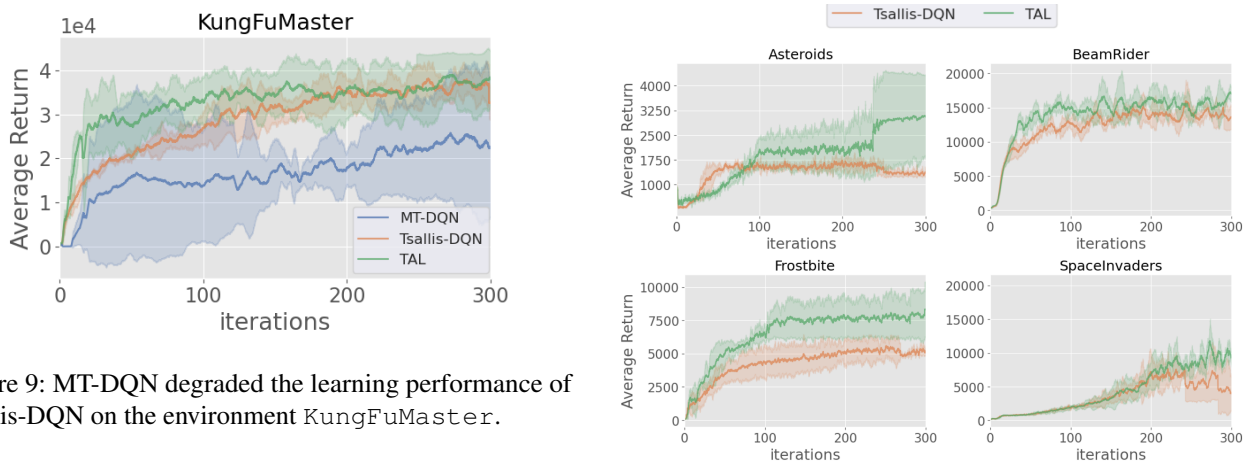


Figure 9: MT-DQN degraded the learning performance of Tsallis-DQN on the environment KungFuMaster.

The learning results in Figure 8 further confirmed our analysis that TAL is robust on complicated environments, and can work well with state-of-the-art RL algorithms. By contrast, MT-DQN failed to learn any meaningful behaviors.

Did TAL improve upon Tsallis-DQN? We compare TAL and Tsallis-DQN on KungFuMaster in which MT-DQN showed non-trivial performance. As illustrated by Figure 9, MT-DQN degraded the performance of Tsallis-DQN, proving the negative effect of the Tsallis Munchausen term. In Figure 10 we compare Tsallis-DQN and TAL, and one can see that TAL still improved upon Tsallis-DQN, which is consistent with the trend shown in Gym and MinAtar environments.

6 DISCUSSION AND CONCLUSION

In this paper we proposed to implicitly perform KL regularization in the maximum Tsallis entropy framework to im-

Figure 10: Comparison between TAL and Tsallis-DQN on four selected Atari games.

prove its error-robustness since the non-Shannon entropies are inherently less robust. We showed simply resorting to recently successful Munchausen DQN led to significantly degraded performance, due to the loss of equivalence between log-policy and advantage learning. Accordingly, a novel algorithm Tsallis advantage learning was proposed to enforce implicit KL regularization. By extensive experiments we verified that TAL improved upon the SOTA value-based MTE method Tsallis-DQN by a large margin, and exhibited comparable performance to SOTA advantage learning methods.

Several interesting future directions include combining TAL with actor-critic methods for further scalability, and leveraging general logarithm function for the Munchausen term so the log-policy term again encodes advantage information.

References

- Zafarali Ahmed, Nicolas Le Roux, Mohammad Norouzi, and Dale Schuurmans. Understanding the impact of entropy on policy optimization. In *Proceedings of 36th International Conference on Machine Learning*, volume 97, pages 151–160, 2019.
- OpenAI: Marcin Andrychowicz, Bowen Baker, Maciek Chociej, and Others. Learning dexterous in-hand manipulation. *The International Journal of Robotics Research*, 39(1):3–20, 2020.
- Mohammad Gheshlaghi Azar, Vicenç Gómez, and Hilbert J Kappen. Dynamic policy programming. *Journal of Machine Learning Research*, 13(1):3207–3245, 2012.
- Leemon Baird and Andrew Moore. Gradient descent for general reinforcement learning. In *Proceedings of the 1998 Conference on Advances in Neural Information Processing Systems II*, page 968–974, 1999.
- Marc G. Bellemare, Yavar Naddaf, Joel Veness, and Michael Bowling. The arcade learning environment: An evaluation platform for general agents. *Journal of Artificial Intelligence Research*, 47(1):253–279, 2013. ISSN 1076-9757.
- Marc G. Bellemare, Georg Ostrovski, Arthur Guez, Philip S. Thomas, and Rémi Munos. Increasing the action gap: New operators for reinforcement learning. In *Proceedings of the AAAI Conference on Artificial Intelligence*, page 1476–1483, 2016.
- Dimitri P Bertsekas and John N Tsitsiklis. *Neuro-Dynamic Programming*. Athena Scientific, 1st edition, 1996. ISBN 1886529108.
- Greg Brockman, Vicki Cheung, Ludwig Pettersson, Jonas Schneider, John Schulman, Jie Tang, and Wojciech Zaremba. Openai gym. *arXiv preprint arXiv:1606.01540*, 2016.
- Gang Chen, Yiming Peng, and Mengjie Zhang. Effective exploration for deep reinforcement learning via bootstrapped q-ensembles under tsallis entropy regularization. *arXiv:abs/1809.00403*, 2018. URL <http://arxiv.org/abs/1809.00403>.
- Yinlam Chow, Ofir Nachum, and Mohammad Ghavamzadeh. Path consistency learning in Tsallis entropy regularized MDPs. In *Proceedings of 35th International Conference on Machine Learning*, volume 80, pages 979–988, 2018.
- Will Dabney, Mark Rowland, Marc Bellemare, and Rémi Munos. Distributional reinforcement learning with quantile regression. In *Proceedings of the AAAI Conference on Artificial Intelligence*, volume 32, pages 2892–2899, 2018.
- Amir-massoud Farahmand. Action-gap phenomenon in reinforcement learning. In *Advances in Neural Information Processing Systems*, pages 1–9, 2011.
- Johan Ferret, Olivier Pietquin, and Matthieu Geist. Self-imitation advantage learning. In *Proceedings of the 20th International Conference on Autonomous Agents and MultiAgent Systems*, AAMAS '21, page 501–509, 2021.
- Justin Fu, Aviral Kumar, Matthew Soh, and Sergey Levine. Diagnosing bottlenecks in deep q-learning algorithms. volume 97 of *Proceedings of 36th International Conference on Machine Learning*, pages 2021–2030, 2019.
- Scott Fujimoto, Herke van Hoof, and David Meger. Addressing function approximation error in actor-critic methods. In *Proceedings of the 35th International Conference on Machine Learning*, volume 80, pages 1587–1596, 2018.
- Matthieu Geist, Bruno Scherrer, and Olivier Pietquin. A theory of regularized Markov decision processes. In *Proceedings of the 36th International Conference on Machine Learning*, volume 97, pages 2160–2169, 2019.
- Tuomas Haarnoja, Aurick Zhou, Pieter Abbeel, and Sergey Levine. Soft actor-critic: Off-policy maximum entropy deep reinforcement learning with a stochastic actor. In *Proceedings of the 35th International Conference on Machine Learning*, volume 80, pages 1861–1870, 2018.
- Tadashi Kozuno, Eiji Uchibe, and Kenji Doya. Theoretical analysis of efficiency and robustness of softmax and gap-increasing operators in reinforcement learning. In *Proceedings of the Twenty-Second International Conference on Artificial Intelligence and Statistics*, volume 89, pages 2995–3003, 2019.
- Kyungjae Lee, Sungjoon Choi, and Songhwai Oh. Sparse markov decision processes with causal sparse tsallis entropy regularization for reinforcement learning. *IEEE Robotics and Automation Letters*, 3:1466–1473, 2018.
- Kyungjae Lee, Sungyub Kim, Sungbin Lim, Sungjoon Choi, Mineui Hong, Jae In Kim, Yong-Lae Park, and Songhwai Oh. Generalized tsallis entropy reinforcement learning and its application to soft mobile robots. In *Robotics: Science and Systems XVI*, pages 1–10, 2020.
- Xiang Li, Wenhao Yang, and Zhihua Zhang. A regularized approach to sparse optimal policy in reinforcement learning. In *Advances in Neural Information Processing Systems 32*, pages 1–11, 2019.
- Yingdong Lu, Mark Squillante, and Chai Wah Wu. A family of robust stochastic operators for reinforcement learning. In *Advances in Neural Information Processing Systems 32*, pages 1–11, 2019.

André F. T. Martins and Ramón F. Astudillo. From softmax to sparsemax: A sparse model of attention and multi-label classification. In *Proceedings of the 33rd International Conference on International Conference on Machine Learning - Volume 48, ICML' 16*, page 1614–1623, 2016.

Volodymyr Mnih, Koray Kavukcuoglu, David Silver, and Others. Human-level control through deep reinforcement learning. *Nature*, 518(7540):529–533, 2015.

Antonin Raffin, Ashley Hill, Adam Gleave, Anssi Kanervisto, Maximilian Ernestus, and Noah Dormann. Stable-baselines3: Reliable reinforcement learning implementations. *Journal of Machine Learning Research*, 22(268): 1–8, 2021.

Constantino Tsallis. Possible generalization of boltzmann-gibbs statistics. *Journal of Statistical Physics*, 52:479–487, 1988.

Nino Vieillard, Tadashi Kozuno, Bruno Scherrer, Olivier Pietquin, Rémi Munos, and Matthieu Geist. Leverage the average: an analysis of regularization in rl. In *Advances in Neural Information Processing Systems 33*, pages 1–12, 2020a.

Nino Vieillard, Olivier Pietquin, and Matthieu Geist. Munchausen reinforcement learning. In *Advances in Neural Information Processing Systems 33*, pages 1–11, 2020b.

Paul Wagner. A reinterpretation of the policy oscillation phenomenon in approximate policy iteration. In *Advances in Neural Information Processing Systems 24*, pages 2573–2581, 2011.

Kenny Young and Tian Tian. Minatar: An atari-inspired testbed for thorough and reproducible reinforcement learning experiments. *arXiv preprint arXiv:1903.03176*, 2019.

A DERIVATION

A.1 DERIVATION OF APPROXIMATE TSALLIS POLICY

The derivation of approximate Tsallis policy basically follows [Chen et al., 2018] but with a general k value instead of $k = 1$.

The derivation begins with assuming an actor-critic framework where the policy network is parametrized by w . It is well-known that the parameters should be updated towards the direction specified by the policy gradient theorem:

$$\Delta w \propto \mathbb{E}_{\pi, d^\pi} \left[Q_\pi \frac{\partial \ln \pi}{\partial w} + \alpha \frac{\partial \mathcal{H}(\pi)}{\partial w} \right] - \sum_s \lambda(s) \frac{\partial \langle \mathbf{1}, \pi \rangle}{\partial w} =: f(w) \quad (12)$$

where d^π denotes the stationary distribution induced by π , $\mathcal{H}(\pi)$ denotes the Shannon entropy and α is the coefficient. $\lambda(s)$ are the Lagrange multipliers for the constraint $\langle \mathbf{1}, \pi \rangle = 1$. In the Tsallis entropy framework, we replace $\mathcal{H}(\pi)$ with $H_q(\pi) := \frac{kq}{q-1} (1 - \langle \mathbf{1}, \pi^q \rangle)$.

We can now explicitly write the optimal condition for the policy network parameters:

$$\begin{aligned} f(w) = 0 &= \mathbb{E}_{\pi, d^\pi} \left[Q_\pi \frac{\partial \ln \pi}{\partial w} + \alpha \frac{\partial H_q(\pi)}{\partial w} \right] - \sum_s \lambda(s) \frac{\partial \langle \mathbf{1}, \pi \rangle}{\partial w} \\ &= \mathbb{E}_{\pi, d^\pi} \left[Q_\pi \frac{\partial \ln \pi}{\partial w} - \alpha \frac{kq}{q-1} \left\langle \mathbf{1}, \pi^q \frac{\partial \ln \pi}{\partial w} \right\rangle - \psi(s) \frac{\partial \ln \pi}{\partial w} \right] \\ &= \mathbb{E}_{\pi, d^\pi} \left[\left(Q_\pi - \alpha \frac{kq}{q-1} \pi^{q-1} - \psi(s) \right) \frac{\partial \ln \pi}{\partial w} \right], \end{aligned} \quad (13)$$

where we leveraged $\frac{\partial H_q(\pi)}{\partial w} = \frac{kq}{q-1} \langle \mathbf{1}, \pi^q \frac{\partial \ln \pi}{\partial w} \rangle$ in the second step and absorbed terms into the expectation with respect to π, d^π in the last step. $\psi(s)$ denotes the adjusted Lagrange multipliers by taking $\lambda(s)$ inside the expectation and modifying it according to the discounted stationary distribution.

Now it suffices to verify either $\frac{\partial \ln \pi}{\partial w} = 0$ or

$$\begin{aligned} Q_\pi(s, a) - \alpha \frac{kq}{q-1} \pi^{q-1}(a|s) - \psi(s) &= 0 \\ \Leftrightarrow \pi^*(a|s) &= \sqrt[q-1]{\left[\frac{Q_\pi(s, a)}{\alpha} - \psi \left(\frac{Q_\pi(s, \cdot)}{\alpha} \right) \right]_+ \frac{q-1}{kq}}. \end{aligned} \quad (14)$$

When $q = 2$, we recover the sparsemax policy Eq. (4) introduced in Section 3.2. When $q \neq 1, 2$, the closed-form expression of π, ψ might not exist. Following [Chen et al., 2018], we leverage first order expansion on the policy as:

$$\tilde{\pi}^*(a|s) \approx 1 + \frac{1}{q-1} \left(\left(\frac{Q_\pi}{\alpha} - \tilde{\psi} \left(\frac{Q_\pi}{\alpha} \right) \right) \frac{q-1}{kq} - 1 \right). \quad (15)$$

By the constraint $\langle \mathbf{1}, \pi \rangle = 1$ we can approximately obtain the normalization as:

$$\tilde{\psi} \left(\frac{Q(s, \cdot)}{\alpha} \right) \approx \frac{\sum_{a \in S(s)} \frac{Q(s, a)}{\alpha} - kq}{K(s)} + \left(kq - \frac{kq}{q-1} \right). \quad (16)$$

The associated set $S(s)$ of allowable actions must satisfy:

$$kq + i \frac{Q_\pi(s, a_{(i)})}{\alpha} \geq \sum_{j=1}^i \frac{Q_\pi(s, a_{(j)})}{\alpha} + j \left(kq - \frac{kq}{q-1} \right). \quad (17)$$

In this paper, we consider the case $k = \frac{1}{2}$, which leads to the following approximate policy and normalization:

$$\tilde{\psi} \left(\frac{Q(s, \cdot)}{\alpha} \right) \approx \frac{\sum_{a \in S(s)} \frac{Q(s, a)}{\alpha} - \frac{1}{2}q}{K(s)} + \left(\frac{q}{2} - \frac{q}{q-2} \right), \quad (18)$$

$$\begin{aligned} \tilde{\mathcal{G}}^\alpha(Q) &\approx 1 + \frac{1}{q-1} \left(\left(\frac{Q}{\alpha} - \tilde{\psi} \left(\frac{Q}{\alpha} \right) \right) \frac{2(q-1)}{q} - 1 \right) \\ &\approx \sqrt[q-1]{\left[\frac{Q}{\alpha} - \tilde{\psi} \left(\frac{Q}{\alpha} \right) \right]_+}. \end{aligned} \quad (19)$$

where the set $S(s)$ then allows actions satisfying $\frac{1}{2}q + i \frac{Q(s, a_{(i)})}{\alpha} > \sum_{j=1}^i \frac{Q(s, a_{(j)})}{\alpha} + j \left(\frac{q}{2} - \frac{q}{q-2} \right)$. We denote its associated Bellman operator as \tilde{T}_π^α .

A.2 ADVANTAGE LEARNING AS KL REGULARIZATION

This section shows our derivation of connection between CVI and MDQN which is different from the connection shown in [Veillard et al., 2020b, Appendix A.4], but our conclusions are essentially the same.

Conservative Value Iteration (CVI) [Kozuno et al., 2019] investigates the scheme maximizing:

$$\mathbb{E} \left[\sum_{t=0}^{\infty} \gamma^t (r_t + \tau \mathcal{H}(\pi(\cdot|s_t)) - \sigma D_{KL}(\pi(\cdot|s_t) \| \bar{\pi}(\cdot|s_t))) \right], \quad (20)$$

where $\mathcal{H}(\pi) := -\langle \pi, \ln \pi \rangle$ is the Shannon entropy and $D_{KL}(\pi \| \bar{\pi}) := \langle \pi, \ln \pi - \ln \bar{\pi} \rangle$ is the KL divergence. By the Fenchel conjugacy, we can show that the optimal policy takes the form

$$\pi^* \propto \bar{\pi}^{\frac{\sigma}{\sigma+\tau}} \exp \left(\frac{1}{\sigma+\tau} (r + \gamma PV_{\bar{\pi}}^*) \right), \quad (21)$$

where $V_{\bar{\pi}}^*$ is the regularized value function. In practice, at the $k+1$ -th iteration, $\bar{\pi}$ is set to the previous

policy π_k . Hence Eq.(21) can be written as $\pi_{k+1} \propto \pi_k^{\frac{\sigma}{\sigma+\tau}} \exp\left(\frac{1}{\sigma+\tau}(r + \gamma PV_{\pi_k})\right)$. While a two-loop policy iteration algorithm can be employed to obtain π_{k+1} , we can avoid computing the recursively defined π_k by defining the action preference function:

$$\Psi_{k+1} := r + \gamma PV_{\pi_k} + \sigma \ln \pi_k = Q_{k+1} + \sigma \ln \pi_k. \quad (22)$$

Now the optimal policy for $k+1$ -th iteration can be compactly expressed as

$$\pi_{k+1} = \frac{\exp\left(\frac{1}{\sigma+\tau}\Psi_{k+1}\right)}{\left\langle \mathbf{1}, \exp\left(\frac{1}{\sigma+\tau}\Psi_{k+1}\right) \right\rangle}. \quad (23)$$

CVI converges to the maximum Shannon entropy optimal policy by iterating upon Ψ :

$$\Psi_{k+1} = r + \gamma P \langle \pi_k, \Psi_k \rangle + \frac{\sigma}{\sigma + \tau} (\Psi_k - W_k), \quad (24)$$

where W_k is the value function associated with Ψ_k and π is a Boltzmann policy. Eq.(24) implies that CVI performs a recursion which evaluates the preference function first: this suggests CVI is different from the conventional value iteration methods such as Eq. (8):

$$\begin{cases} \Psi_{k+1} = r + \gamma P \langle \pi_k, \Psi_k \rangle + \frac{\sigma}{\sigma+\tau} (\Psi_k - W_k) \\ \pi_{k+1} = \exp\left(\frac{1}{\sigma+\tau}\Psi_{k+1}\right) / \left\langle \mathbf{1}, \exp\left(\frac{1}{\sigma+\tau}\Psi_{k+1}\right) \right\rangle \end{cases}, \quad (25)$$

Without loss of generality we can reverse the order in Eq. (25) by assuming π_0 is a uniform policy:

$$\begin{cases} \pi_{k+1} = \exp\left(\frac{1}{\sigma+\tau}\Psi_k\right) / \left\langle \mathbf{1}, \exp\left(\frac{1}{\sigma+\tau}\Psi_k\right) \right\rangle, \\ \Psi_{k+1} = r + \gamma P \langle \pi_{k+1}, \Psi_k \rangle + \frac{\sigma}{\sigma+\tau} (\Psi_k - W_k), \end{cases} \quad (26)$$

where the definition of the action preference function is modified as:

$$\Psi_{k+1} := Q_{k+1} + \sigma \ln \pi_{k+1}. \quad (27)$$

We see if we set $\beta := \frac{\sigma}{\sigma+\tau} \in [0, 1]$ and $\zeta := \frac{1}{\sigma+\tau} \in (0, \infty]$ in Eq. (26), we obtain Eq. (10). Hence the CVI recursion can now be rewritten as:

$$\Psi_{k+1} = r + \gamma P \langle \pi_{k+1}, \Psi_k \rangle + \beta (\Psi_k - W_k). \quad (28)$$

It is worth noting that Eq. (28) is itself a new value iteration scheme, regardless of the definition of Ψ . CVI states that, if the policy satisfies the Boltzmann assumption, then simply iterating upon Eq. (28) results in KL regularization.

The above analysis implies that any value iteration methods could enjoy the KL regularization properties by replacing Ψ, W with Q, V without needing to care about the definition of Ψ, W since we can arbitrarily initialize $Q_0 = \Psi_0 = 0$.

The simplest method to ensure the policy meets the Boltzmann assumption is by performing soft Q-learning on top of Eq. (28). By rewriting Eq. (28) as a soft Q-learning scheme and replacing every appearance of Ψ, W with Q, V , we have:

$$Q_{k+1} = r + \beta(Q_k - V_k) + \gamma P \langle \pi_{k+1}, Q_k - \tau \ln \pi_{k+1} \rangle, \quad (29)$$

where the blue part is due to the definition of soft Q-learning as in Eq. (8) to ensure the policy is a Boltzmann distribution. By observing that $\beta(Q_k - V_k) = \beta\tau \ln \pi_k$ we see this is the Munchausen DQN update rule Eq. (8).

The key for deriving the relationship between CVI and MDQN is the equivalence $\tau \ln \pi_{k+1} = Q_k - V_k$. It is hence natural to conjecture that, if the equivalence does not hold as when $q \neq 1$ in the general Tsallis entropy, MDQN can no longer perform implicit KL regularization. Furthermore, the contraction property might be lost by adding such $\ln \pi$ term.

A.3 TSALLIS ADVANTAGE LEARNING FOR KL REGULARIZATION

In Section A.2 we analyzed the relationship between advantage learning and KL regularization. In practice, the value function W_k in CVI recursion Eq. (24) is approximated by $\langle \pi_k, \Psi_k \rangle$ as it saves computation and achieves numerical stability [Azar et al., 2012, Kozuno et al., 2019]. The requirement of π being Boltzmann distribution is not a must, as can be seen from [Kozuno et al., 2019, Eq. (12)] which states that any policy μ_k satisfying the relation $\langle \mu_k, \Psi_k \rangle \geq \langle \pi_k, \Psi_k \rangle$ can be used. This constitutes the theoretical basis for our use of $\langle \pi_k, Q_k \rangle$ in Eq. (11) at the absence of analytic value function expression. Even for $q = 2$ where the closed-form V is available, we found that using the advantage as $Q_k - \langle \pi_k, Q_k \rangle$ significantly improved the performance and stability.

B IMPLEMENTATION DETAILS

In this section we provide implementation details for all environments we used. Specifically, three different architectures were leveraged for handling gym environments, MinAtar games and Atari games, detailed in Sections B.1, B.2 and B.3, respectively. We added a small number Δ to π to ensure $\ln \pi$ is well defined. For fast and reproducible evaluation, we implemented all algorithms based on the Stable-Baselines3 library [Raffin et al., 2021].

B.1 GYM CLASSIC CONTROL

We introduce the parameters we used for the Gym environments in this section. Specifically, the hyperparameters are listed in Table 1. The epsilon threshold is fixed at 0.01

from the beginning of learning. The Munchausen number Δ refers to the small value added to the policy to prevent ill-defined $\ln \pi$. FC n refers to the fully connected layer with n activation units.

Table 1: Parameters used for TAL, MT-DQN and Tsallis-DQN on `CartPole-v1` and `LunarLander-v2`.

Parameter	Value
T (total steps)	5×10^5
C (interaction period)	4
$ B $ (buffer size)	5×10^4
B_t (batch size)	128
γ (discount rate)	0.99
I (update period)	1000 (Car.) / 2500 (Others)
ϵ (epsilon greedy threshold)	0.01
Δ (Munchausen number)	10^{-8}
α (Tsallis entropy coefficient)	0.03
β (advantage coefficient)	0.99
Q-network architecture	FC512 - FC512
activation units	ReLU
optimizer	Adam
optimizer learning rate	10^{-3}

B.2 MINATAR GAMES

For MinAtar games we employed the configuration recommended by [Young and Tian, 2019]. The hyperparameters are listed in Table 2.

Since MinAtar games optimize different aspects of Atari games, no frame skipping is necessary and hence the for every frame we update the network. The epsilon greedy threshold $\epsilon : 1.0 \rightarrow 0.05|_{10\%}$ denotes that ϵ is initialized as 1.0 and gradually decays to 0.05 through the first 10% of learning.

The parameter τ is the Shannon entropy coefficient used for MDQN and plays a similar role as α . The advantage learning coefficient β is also used for PAL. For SAL, we use the empirically most performant choice β_{SAL} of [Lu et al., 2019] which is drawn from the Beta(2, 9) distribution and adds a constant $\frac{7}{9}$. Then $\mathbb{E}[\beta_{\text{SAL}}] = 1$ and $\text{Var}[\beta_{\text{SAL}}] = \frac{7}{405}$.

The network architecture consists of only one convolutional layer where $\text{Conv}_{a,b}^d$ denotes a convolutional layer with c filters of size $a \times b$ and stride d .

In Appendix A.2 we analyzed the relationship between MDQN and CVI and in Figure 7 we compared TAL against CVI and TAL with entropic index $q = 2$ to see if TAL can achieve comparable performance to the state-of-the-art algorithm. CVI used the same Boltzmann temperature $\frac{1}{\sigma + \tau} = 0.03$ and advantage coefficient β as in Table 2. Since CVI and TAL exhibited similar performance, it might be safe to replace the Shannon entropy with Tsallis entropy in many applications where safety or parsimonious descrip-

Table 2: Parameters used for TAL, MT-DQN, Tsallis-DQN, PAL, SAL and MDQN on all MinAtar games.

Parameter	Value
T (total steps)	1×10^7
C (interaction period)	1
$ B $ (buffer size)	1×10^5
B_t (batch size)	32
γ (discount rate)	0.99
I (update period)	1000
ϵ (epsilon greedy threshold)	$1.0 \rightarrow 0.05 _{10\%}$
Δ (Munchausen number)	10^{-8}
α (Tsallis entropy coefficient)	0.03
τ (Munchausen entropy coefficient)	0.03
β (advantage coefficient)	0.9
β_{SAL} (SAL advantage coefficient)	Beta(2, 9) + $\frac{7}{9}$
Q-network architecture	Conv $_{3,3}^1$ 16 - FC128
activation units	ReLU
optimizer	RMSProp
optimizer learning rate	2.5×10^{-4}
(RMSProp) squared momentum	0.95
(RMSProp) minimum momentum	0.01

tion of the action space are necessary [Lee et al., 2018], since the maximum Shannon entropy policy always assigns non-negligible probabilities to sub-optimal or even unsafe actions.

Table 3: Parameters used for distributional TAL, MT-DQN and Tsallis-DQN on Atari games.

Parameter	Value
T (total steps)	3×10^7
C (interaction period)	4
$ B $ (buffer size)	1×10^6
B_t (batch size)	32
γ (discount rate)	0.99
I (update period)	8000
ϵ (epsilon greedy threshold)	$1.0 \rightarrow 0.01 _{10\%}$
Δ (Munchausen number)	10^{-8}
α (Tsallis entropy coefficient)	10
β (advantage coefficient)	0.9
Q-network architecture	Conv $_{8,8}^4$ 32 - Conv $_{4,4}^2$ 64 - Conv $_{3,3}^1$ 64 - FC512 - FC
activation units	ReLU
optimizer	Adam
optimizer learning rate	10^{-4}

B.3 ATARI GAMES

We implemented TAL and MT-DQN on top of QR-DQN, which is a famous distributional RL algorithm. Instead of learning the conditional expectation of cumulative return Q as in Eq. (1), distributional RL attempts to learn the distribu-

tion itself:

$$\begin{aligned} Q_\pi(s, a) &= \mathbb{E}[Z_\pi(s, a)], \\ T_\pi Z(s, a) &= r(s, a) + \gamma Z(s', a'). \end{aligned} \tag{30}$$

Specifically, QR-DQN aims to approximate Z via quantile regression by parametrizing fixed probabilities (quantiles). Based on QR-DQN, TAL and MT-DQN are implemented by replacing Q with Z in Eq. (4).

For the full-fledged Atari games learning is more challenging than the optimized MinAtar games. We leverage the optimized Stable-Baselines3 architecture [Raffin et al., 2021] for best performance. The details can be seen from Table 3. The Q-network uses 3 convolutional layers. The epsilon greedy threshold is initialized at 1.0 and gradually decays to 0.01 at the end of first 10% of learning. For conservative learning, we choose the Tsallis entropy coefficient as $\alpha = 10$.